High speed CO2 laser surface modification of iron/cobalt co-doped boroaluminosilicate glass and the impact on surface roughness, gloss and wettability

Hodgson, SD, Waugh, DG, Gillett, A & Lawrence, J

High speed CO₂ laser surface modification of iron/cobalt co-doped boroaluminosilicate glass and the impact on surface roughness, gloss and wettability.

S. D. Hodgson[a]*, D. G. Waugh[a], A. Gillett[a], J. Lawrence[a]

[a]Laser Engineering and Manufacturing Research Centre, Faculty of Science and Engineering, University of Chester, Parkgate Road, Chester, CH1 4BJ.

Corresponding Author e-mail: s.hodgson@chester.ac.uk

Abstract

A preliminary study into the impact of high speed laser processing on the surface of iron and cobalt co-doped glass substrates using a 60 W continuous wave (cw) CO₂ laser. Two types of processing, termed fill-processing and line-processing, were trialled. In fill-processed samples the surface roughness of the glass was found to increase linearly with laser power from an S_a value of 20.8 nm to 2.1 μm at a processing power of 54 W. With line processing, a more exponential-like increase was observed with a roughness of 4 μm at 54 W. The change in surface properties of the glass, such as gloss and wettability, have also been measured. The contact angle of water was found to increase after laser processing by up to 64°. The surface gloss was varied between 45 and 100 gloss units (GUs).

Keywords: CO₂ Laser, Materials processing, Glass, Surface Roughness, Gloss Measurement.

Introduction

The term laser materials processing describes a massively varied range of techniques that alter the surface properties of a material. Materials processing can include, without being limited to, surface modification [1], cutting [2], welding [3], drilling [4] and peening [5]. Lasers are highly versatile, with different technologies being capable of emitting light at different wavelengths (including ultra-violet, visible and infra-red [6, 7]) as well as emitting light as either a constant beam or in pulses ranging from milliseconds to attoseconds [8, 9]. For the purpose of rapid surface processing, the CO₂ laser offers two primary advantages; firstly it is an efficient laser source that is capable of operating as a continuous wave at high power, and secondly, CO₂ lasers emit light at a wavelength of approximately 10.6 μm, which is in the long-wavelength infra-red (LWIR) region. Whilst this long wavelength makes the creation of high resolution nanostructured surfaces very difficult, the continuous wave-nature of the laser lends itself to very high-speed processes. This helps to make the CO₂ laser highly versatile, able to be used in industrial scale production as well as in smaller-scale laboratories.

Glass is found in an ever increasing array of technological applications. The ability to tune both its properties and appearance through the introduction (or removal) of impurity elements has led to it being used in such advanced industries as optoelectronics, construction, medical, automotive and aerospace [10-15]. Its versatility lends itself to high end technologies and it is also used in artwork

and other aesthetic based mediums [16]. The most common type is soda-lime glass which is low in cost and quite stable with good mechanical properties [17]. By adding lead oxide to the glass, or other metal oxides such as titanium or barium (flint glass) which are less toxic, the refractive index (RI) can be increased. This increases the reflective and refractive properties of the glass and is useful in optical applications such as prisms or focusing lenses [18]. The addition of boron trioxide (B_2O_3) to form borosilicate glass lowers the coefficient of thermal expansion making it more stable when subjected to temperature changes [19]. Additionally the absence of certain impurities (such as Iron) increases the optical transparency making it well suited for use in industries like photovoltaics where the glass may be subjected to high temperatures during semiconductor deposition and require as much light as possible to pass through to the absorber layer [20]. It is also well suited to technologies requiring increased infra-red transparency [21]. To modify the colour of glass there are several elemental impurities that can be added. Iron, chromium, cobalt, manganese and sulphur are examples of elements that, either individually, combined or as oxides act to alter the colour of glass [22].

Gloss measurements provide information on the reflectivity of a material at certain angles. The level of gloss is heavily influenced by the RI of the material and the surface topography (i.e. roughness and features). Glossmeters, whilst lacking the diversity of measurement of spectrophotometers, provide quick useful information on properties such as the amount of specular reflection, sheen and haze of a material [23]. This is of significant interest for those companies working in the coatings and surface industries. These include paints and surface finish industries which directly link to industries such as the automotive industry and the aerospace industry.

The wettability of a material describes its adhesive contact with a liquid. In terms of water this describes the hydrophobicity or hydrophilicity of the surface. The level of wetting comes about through the balance of the adhesive forces of the liquid droplet to the surface and the cohesive forces of the molecules within the droplet. When a droplet is placed on a surface there are three possible outcomes: complete wetting, complete dewetting, and partial wetting. The degree to which wetting as occurred is obtained by measuring the contact angle of the droplet relative to the surface where the greater the contact angle, the greater the degree of wetting [24, 25]. The wettability of glass is of particular importance to the automotive industry where visibility, particularly under extreme weather conditions, through control of water run-off is key. Wettability of glass is also linked with self-cleaning phenomena, a property important for outdoor usage [26].

This study demonstrates the effect of CO_2 laser surface treatment of this type of doped-glass and discusses the effect of laser-induced roughness and surface feature on the surface gloss and wettability properties.

Experimental

Laser Materials Processing: A continuous wave (cw) 60W Synrad Firestar CO_2 laser marking system was used for the surface processing. Several processing parameters were changed over the course of this study. These included laser output power, processing speed, type of processing (whole area or a series of spaced lines) and the line spacing. Areas of 15×15 mm^2 in size were processed for each change in parameter and before processing, the glass samples were cleaned using a dry-rub with a lint-free cloth. All surface treatment was carried out in ambient air.

A range of processing parameters have been tested and are summarised in table 1. Two types of laser patterns, referred to as line (equally spaced lines marked as vectors) and fill (an area filled as a raster pattern with individual lines designed to overlap slightly thus presenting the filled area). For both of these, the power was varied from 10 % (6 W) to 90 % (54 W) with scanning speed and line spacing held constant (480 mm/s and 0.4 mm respectively). Additionally power and spacing have been held constant with processing speed varied and speed and power held constant with line spacing varied. Each of the laser processed areas was 15×15 mm^2.

Table 1: Laser parameters for the surface treatment of glass.

Power (W)	6	18	30	42	54		30	30	30	30	30	30
Processing Speed (mm/s)	480	480	480	480	480		60	120	240	480	720	960
Line Spacing (mm)	N/A	N/A	N/A	N/A	N/A		0.4	0.4	0.4	0.4	0.4	0.4
Power (W)	6	18	30	42	54	30	30	30	30	30	30	30
Processing Speed (mm/s)	480	480	480	480	480	480	480	480	480	480	480	480
Line Spacing (mm)	0.4	0.4	0.4	0.4	0.4	0.05	0.1	0.2	0.4	0.6	0.8	1.0

Characterisation: Surface roughness was characterised using a STIL Micromeasure 2 white light confocal chromatic imager (CCI). S$_a$, the roughness parameter measured in this study, is the arithmetic mean of the surface roughness and can be calculated using equation 1:

$$S_a = \iint_a |Z_{(X,Y)}| \, dx \, dy \qquad (1)$$

The IR spectrum of the glass was taken using a Varian Scimitar 2000 spectrometer using an Attenuated Total Reflectance (ATR) measurement type. The ATR crystal used was zinc selenide. Gloss measurements were obtained at three angles (20°, 60° and 85°) using an Elcometer 480 glossmeter. Wettability measurements were obtained using a Dataphysics OCA20 contact angle goniometer with deionised water as the test liquid. For each sample, 10 measurements were performed and the mean contact angle taken.

Results and Discussion

Laser Surface Modification

In order for the CO_2 laser to be able to mark the surface of a material, it must be able to couple into the target material. The Synrad CO_2 laser emits at wavelengths between 10.55 – 10.68 µm, and to confirm whether or not the laser is suitable for processing the doped glass it was possible to measure the IR spectrum of the material (see Figure 1). Figure 1 shows the doped glass allowed only a very small amount of light to pass through at the laser's emission range. This is indicative of a significant portion of the light interacting with the surface (either through absorption or reflection),

which is suggestive that the laser coupled well into the glass. For an infra-red laser such as the CO_2 laser used in this work, the laser would have activated the vibrational modes of the glass molecules heating the sample sufficiently to induce a localised melt.
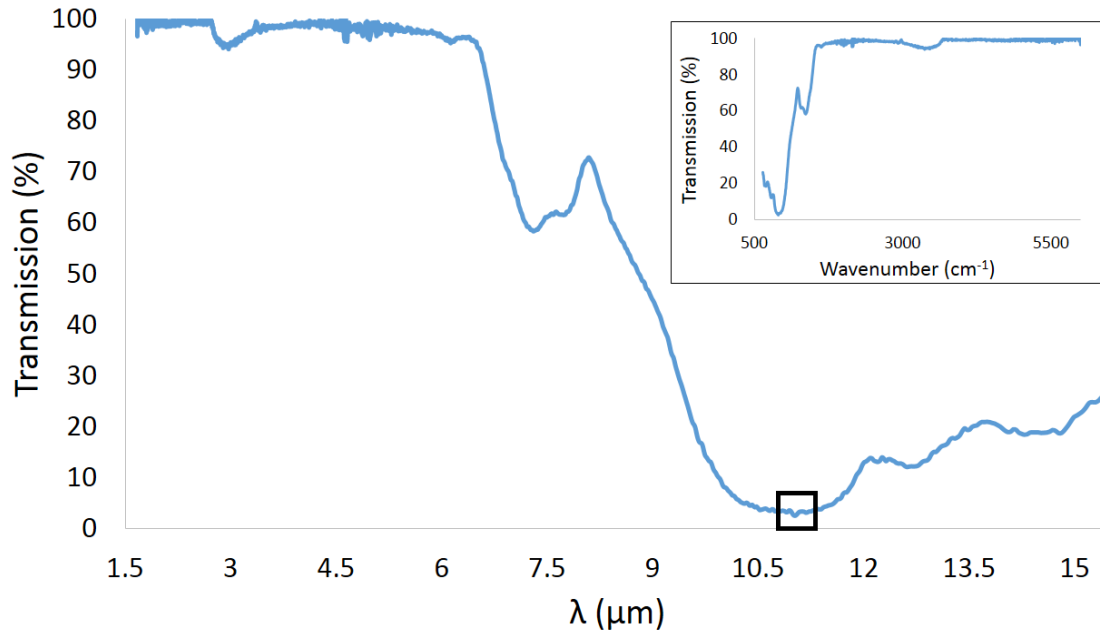

Figure 1: ATR-IR spectrum of the doped-glass showing low transmissivity of light at the wavelength typical of a CO_2 laser (area within black box). Inset graph: The same spectrum plotting transmission against the more conventional unit of wavenumbers.

Optical microscopy of the laser scribes can be found in Figure 2. For fill-processed samples the increase in laser-power increased the definition of the visible melt to the surface. In some cases there is some light visible cracking (1b, 2b, 2c, 3a, 4b, 4c). The cracking varies in length and width, although always appears to be < 10 µm in width, however this is inconsistent from sample to sample suggesting that it may be down to the unique composition of the particular section of glass rather than the laser parameters. Another phenomenon that may have been occurring at higher powers is remelting of cracks in the surface due to overlapping of the rastored lines. Increasing the power of the line-processed slides increases the depth of the scribe, again at higher powers cracking is visible on some of the samples. Varying the processing speed affects the scribe width. The slower the speed the more width to the scribe. This will be due to the longer dwell time per-spot of the laser. Increasing the spacing of the lines has limited effect on the individual scribe. However at low scribe spacing the surface takes on an appearance more resembling that of the fill-processed samples. This is due to the spacing being of a level similar to that of the beam width (~95 µm).
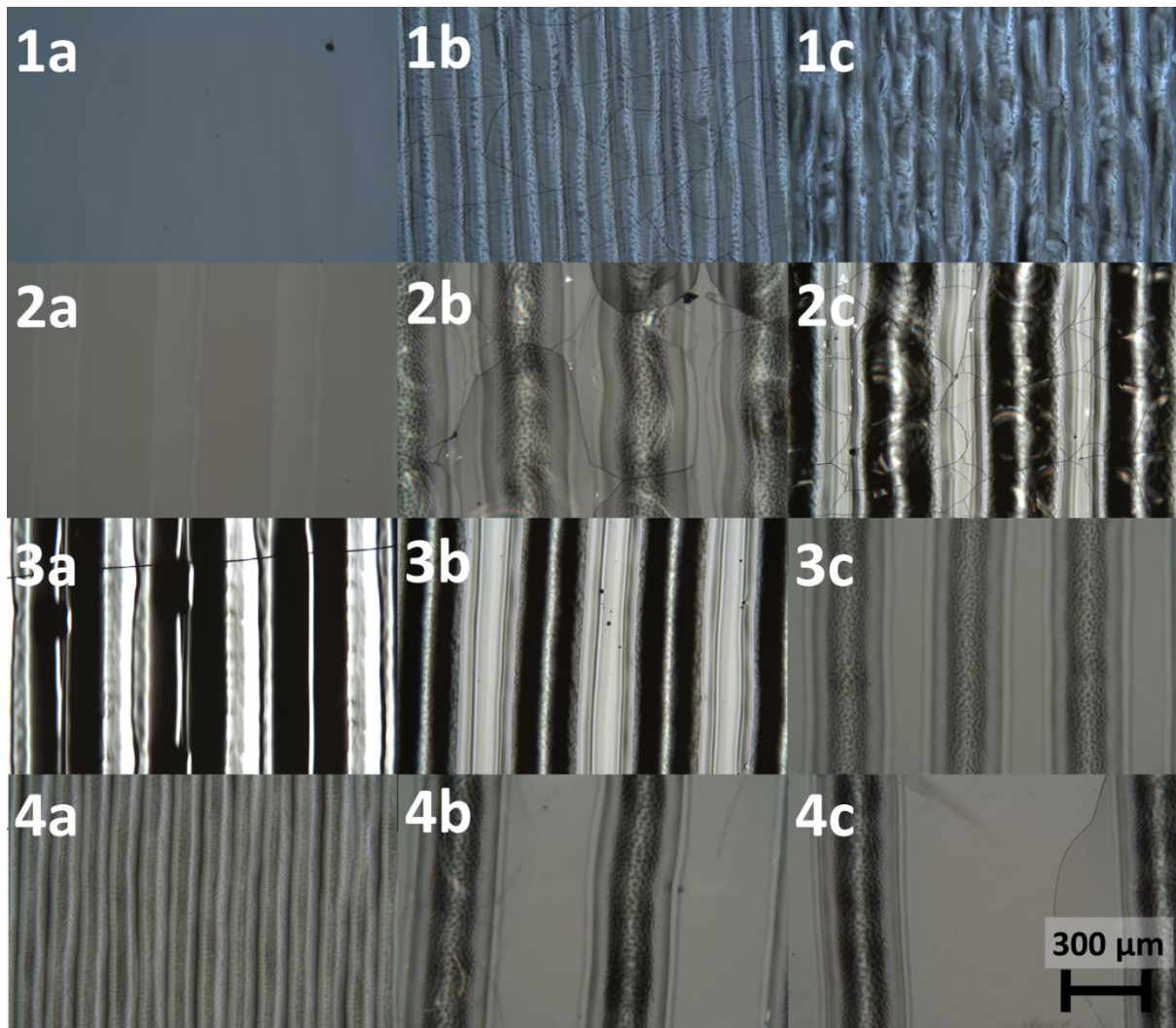
Figure 2: Optical micrographs at 100x magnification of a selection of the laser-treated glass. Samples 1a-c have been fill (rastor) processed at 10, 50 and 90% power. Samples 2a-c are equivalent in power to row 1 but line (vector) processed. Samples 3a-c have varying processing speeds of 60, 240 and 720 mm/s. Row 4a-c are processed with varying line-widths of 0.1, 06 and 1 mm. The scale bar indicates 100 µm. All samples 3 (a-c) and 4 (a-c) are line processed.

Optical Profilometry

By using a CCI to optically measure the surfaces of the laser-processed glass it was possible to calculate the surface roughness (S_a). Figure 3 shows a selection of the surface profiles. The surface profiles confirm the trends to those observed with the optical microscopy such as wider scribes with reduced processing speed. In addition to this, Figure 3 confirms the periodicity of the pattern induced by the CO_2 laser.

 The calculated surface roughness values for each processing sequence are included in Figure 4. For fill-processed samples, there is a linear increase (R^2 fit of 0.94) with surface roughness increasing with laser power. This can be explained by the increased power of the laser resulting in increased ablation and re-melting of the glass surface. For line-processed films there is a similar trend for

lower powers however the overall fit is an exponential curve (R^2 fit of 0.92) due to a drastic increase in surface roughness at higher powers (although the S_a for all the line processed samples is slightly higher than the fill processed equivalent). The general roughness increase could be due to the appearance of a heat affected zone (HAZ) between scribe lines, something that will be effectively be absent from the fill processed samples due to the reprocessing of the HAZ by the next pass of the beam. At higher powers the laser appears to have caused pitting, something that may be absent from the fill processing due to remelting effects. Slow processing speeds triggered high roughness; again this is likely down to the dwell time of the laser on the substrate causing greater melting and re-solidification. Once the processing speed crosses a threshold there was no real change in the surface roughness. There was also no trend in the change of S_a with the line spacing samples.
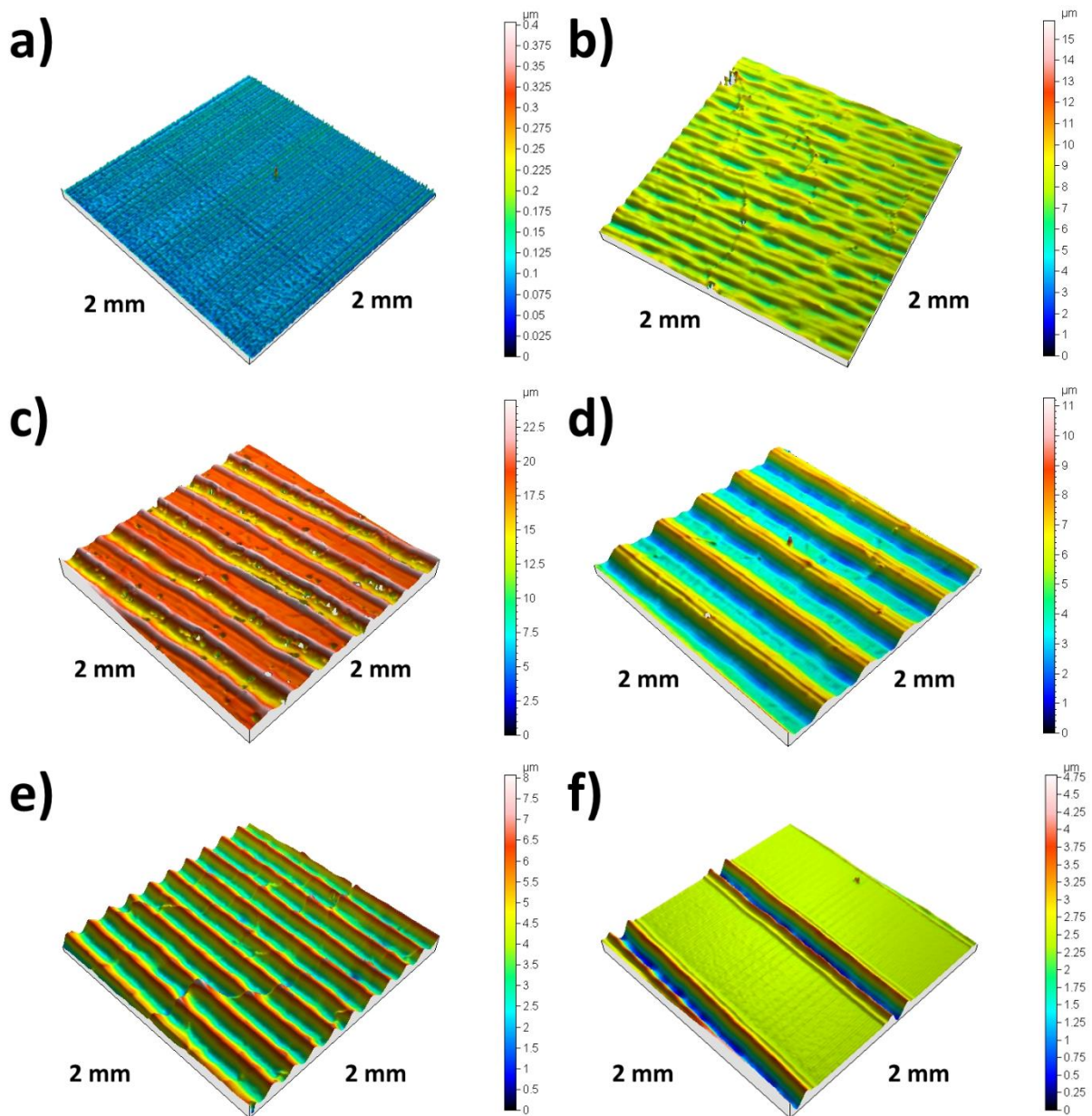

Figure 3: Surface topography of selected laser processed samples taken using CCI. The samples are: a) unprocessed glass, b) 42 W power fill-processed, c) 42 W power line-processed 480 mm/s

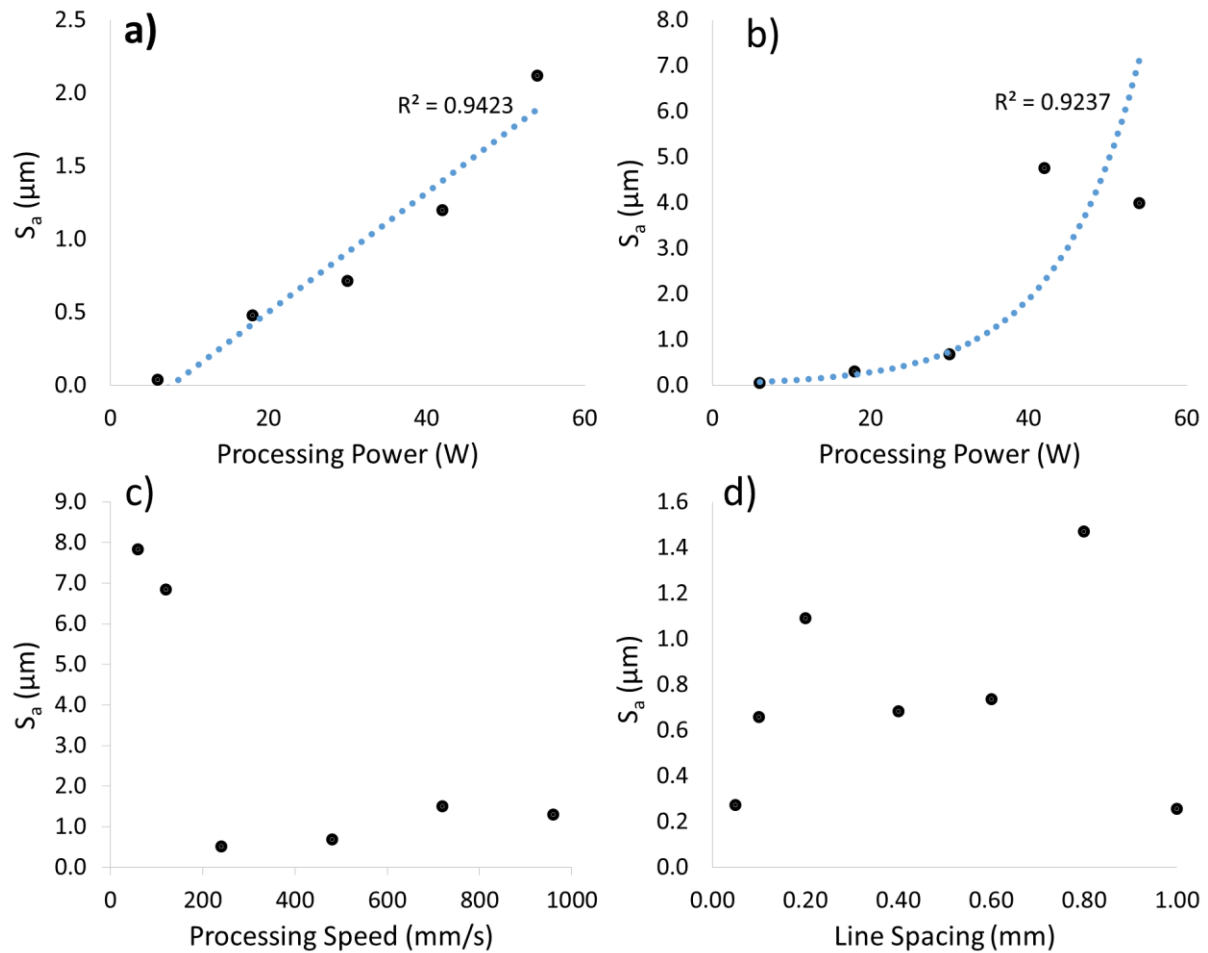processing speed, d) 120 mm/s processing speed, e) 0.2 mm line spacing, and f) 1mm line spacing. Each sample is a 2×2 mm^2 area.

Figure 4: Graphs of surface roughness values (S_a) against laser processing parameters as calculated from 3D CCI scans (optical profilometry). Graph a) fill processing, b) line processing, c) processing speed, d) line spacing. For reference the S_a of untreated glass was 20.8 nm.

Gloss

As mentioned, the gloss measurement is highly dependent on the topography of the surface [23]. As such, the introduction of line-processing showed no trends in relation to either processing speed, line spacing or surface roughness. This is presumably due to the periodic surface structure creating more diffuse scattering of light. On the fill-processed samples, at low-mid angles (angles relative to the perpendicular of the surface) the level of specular reflection decreased linearly as the surface roughness increases (as shown in Figure 4a roughness increases linearly for fill processed samples). This is likely due to an increase in roughness corresponding to an increase in diffuse reflection of light and relates to the pitting observed at higher laser powers. At the highest measured angle, there

was no trend even on these samples. Again this was likely due to even small surface features dominating over specular reflection, this is shown in Figure 5a. Further analysis using transmission spectroscopy would provide more information on the type and amount of reflection occurring.

Wettability

Many glass surfaces are exposed to water, so the ability to modify the relative hydrophilicity or hydrophobicity of glass surfaces is of great importance. On each of the samples the contact angle of water drops were measured on the CO_2 laser processed glass. The CO_2 laser processing of the surface (Figure 5b) resulted in an initial decrease in the contact angle of the water from its initial value of 85.9° to a low of 21.8°. With an initial contact angle of 85.9° the glass surface can be classified as slightly hydrophilic, thus the CO_2 laser processing is increasing the hydrophilicity of the surface. This CO_2 laser-processing induced an initial decrease stabilising between 20 and 30 W of laser power before the contact angle began to increase again (albeit staying below the initial value). This demonstrates that CO_2 laser processing at comparatively low powers can cause a significant increase in the adhesion properties of this type of glass (a decrease in contact angle of up to 64.1°). Line processing demonstrated a similar effect to that seen with the fill processed samples. The laser processed lines, when compared with the fill processed samples, gave rise to greater adhesion properties at low laser powers and reduced contact angle recovery at higher powers. The processing speed and spacing of lines showed no consistent influence on the measured contact angle. This is likely due to variations in the surface properties arising from the laser-material interaction between the laser and the non-uniform, non-homogenous iron/cobalt co-doped boroaluminosilicate glass samples.
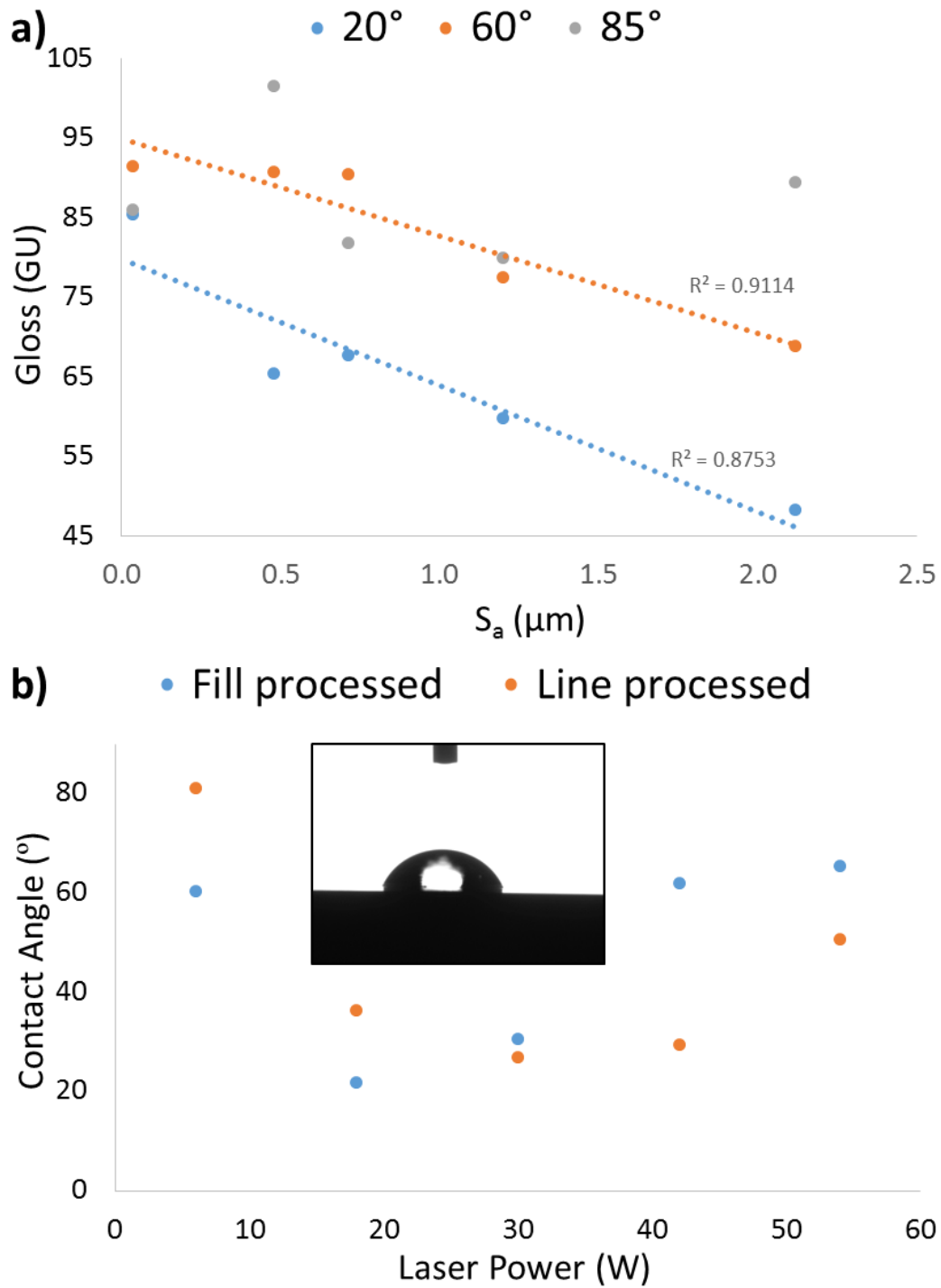
Figure 5: a) A plot of gloss against surface roughness for the fill processed samples. b) A plot of contact angle (for water) against laser power for area and line processed samples (INSET: A water droplet on the doped glass). The contact angle for the unprocessed glass was measured at 85.9°.

Conclusions

The surface of co-doped glass has been successfully modified by high speed CO_2 laser processing. By controlling the power of the laser the surface roughness can be tuned and the introduction of line

processing shows generally increased surface roughness up to a maximum achieved S_a value of 7.8 μm. Attempts to tune the parameters of the line-processed samples, by varying processing speed and line spacing, showed no consistent change in the roughness of the surface. Useful surface properties such as the gloss and wettability (relative to water) have also been measured. The wettability was found to vary with laser power, with only a relatively low laser power being sufficient to decrease the contact angle (i.e. increase the wettability). Line processing showed a similar, albeit slightly reduced effect. The laser processing reduced the gloss of the sample at all three angles of reflection measured, with a linear decrease (in proportion to surface roughness) at low-mid angles. At the greatest angle, there was no consistent trend in gloss values suggesting that at low angles any surface features present are sufficient to limit the specular reflection. Line processing showed no consistent trend in the gloss, again suggesting the greater significance of the effect of surface features over general surface roughness. Further work improving on the results of this preliminary study is needed to better understand the relationship between the laser processing and the gloss/wettability of the glass.

References

[1] D.G. Waugh, J. Lawrence, D.J. Morgan, C.L. Thomas, Interaction of CO2 laser-modified nylon with osteoblast cells in relation to wettability, Materials Science & Engineering C-Materials for Biological Applications, 29 (2009) 2514-2524.
[2] D. Schindhelm, R. Weber, T. Graf, Spatial analysis of the back reflected laser light during CO2-laser cutting of metal sheets, Journal of Laser Applications, 25 (2013).
[3] J.T. Norris, C.V. Robino, D.A. Hirschfeld, M.J. Perricone, Effects of Laser Parameters on Porosity Formation: Investigating Millimeter Scale Continous Wave Nd:YAG Laser Welds, Welding Journal, 90 (2011) 198S-203S.
[4] Y. Wu, A.H. Wang, R.R. Zheng, H.Q. Tang, X.Y. Qi, B. Ye, Laser-drilled micro-hole arrays on polyurethane synthetic leather for improvement of water vapor permeability, Applied Surface Science, 305 (2014) 1-8.
[5] P.P. Shukla, P.T. Swanson, C.J. Page, Laser shock peening and mechanical shot peening processes applicable for the surface treatment of technical grade ceramics: A review, Proceedings of the Institution of Mechanical Engineers Part B-Journal of Engineering Manufacture, 228 (2014) 639-652.
[6] Z. Banihashemi, J.D. MacDonald, M.C. Lagunas-Solar, Effect of high-power monochromatic (pulsed UV laser) and low-power broadband UV radiation on Phytophthora spp. in irrigation water, European Journal of Plant Pathology, 127 (2010) 229-238.
[7] C. Becker, T. Oesselke, J. Pandavenes, R. Ricken, K. Rochhausen, G. Schreiber, W. Sohler, H. Suche, R. Wessel, S. Balsamo, I. Montrosset, D. Sciancalepore, Advanced Ti : Er : LiNbO3 waveguide lasers, Ieee Journal of Selected Topics in Quantum Electronics, 6 (2000) 101-113.

[8] C. Vozzi, E. Calegari, E. Ferrari, M. Lucchini, S. De Silvestri, O. Svelto, G. Sansone, S. Stagira, M. Nisoli, Advances in laser technology for isolated attosecond pulse generation, Laser Physics Letters, 6 (2009) 259-267.

[9] X. Wang, D.H. Zhu, Z.H. Shen, J. Lu, X.W. Ni, Surface damage morphology investigations of silicon under millisecond laser irradiation, Applied Surface Science, 257 (2010) 1583-1588.

[10] M.N.C. Grainger, M. Manley-Harris, S. Coulson, Classification and discrimination of automotive glass using LA-ICP-MS, Journal of Analytical Atomic Spectrometry, 27 (2012) 1413-1422.

[11] T. Maeder, Review of Bi2O3 based glasses for electronics and related applications, International Materials Reviews, 58 (2013) 3-40.

[12] K. Swapna, S. Mahamuda, A.S. Rao, M. Jayasimhadri, T. Sasikala, L.R. Moorthy, Visible fluorescence characteristics of Dy3+ doped zinc alumino bismuth borate glasses for optoelectronic devices, Ceramics International, 39 (2013) 8459-8465.

[13] B. Siebert, I. Maniatis, Glass constructions - Applications in Germany, Challenging Glass, (2008) 119-125.

[14] M. Vallet-Regi, C.V. Ragel, A.J. Salinas, Glasses with medical applications, European Journal of Inorganic Chemistry, (2003) 1029-1042.

[15] K.K. Tedjojuwono, N. Clark, W.M. Humphreys, Optical Characterization of Window Materials for Aerospace Applications, in: Conference on Optifab, Spie-Int Soc Optical Engineering, Rochester, NY, 2013.

[16] M.d.C. Dominguez Rodes, S. Canellas Martinez, Materials for stained glass windows in catalonian documentation (14th and 15th centuries), Journal of Cultural Heritage, 9 (2008) E85-E88.

[17] E. Kilinc, R.J. Hand, Mechanical properties of soda-lime-silica glasses with varying alkaline earth contents, Journal of Non-Crystalline Solids, 429 (2015) 190-197.

[18] G. Gupta, M. Sugimoto, Y. Matsui, J. Kondoh, Use of a low refractive index prism in surface plasmon resonance biosensing, Sensors and Actuators B-Chemical, 130 (2008) 689-695.

[19] H. Darwish, S.N. Salama, S.M. Salman, Contribution of germanium dioxide to the thermal expansion characteristics of some borosilicate glasses and their corresponding glass-ceramics, Thermochimica Acta, 374 (2001) 129-135.

[20] Y.S. Khoo, T.M. Walsh, A.G. Aberle, Novel Method for Quantifying Optical Losses of Glass and Encapsulant Materials of Silicon Wafer Based PV Modules, Energy Procedia, 15 (2012) 403-412.

[21] X.H. Zhang, L. Calvez, V. Seznec, H.L. Ma, S. Danto, P. Houizot, C. Boussard-Pledel, J. Lucas, Infrared transmitting glasses and glass-ceramics, Journal of Non-Crystalline Solids, 352 (2006) 2411-2415.

[22] K. Gerth, D. Schops, K. Heide, E. Woermann, Investigation of coloured glasses from the cathedral of aachen by methods of geochemistry and glass-chemistry, Chemie Der Erde-Geochemistry, 60 (2000) 67-80.

[23] F.B. Leloup, G. Obein, M.R. Pointer, P. Hanselaer, Toward the Soft Metrology of Surface Gloss: A Review, Color Research and Application, 39 (2014) 559-570.

[24] M. Mohammed, T. Babadagli, Wettability alteration: A comprehensive review of materials/methods and testing the selected ones on heavy-oil containing oil-wet systems, Advances in Colloid and Interface Science, 220 (2015) 54-77.

[25] T. Watanabe, Wettability of ceramic surfaces -A wide range control of surface wettability from super hydrophilicity to super hydrophobicity, from static wettability to dynamic wettability, Journal of the Ceramic Society of Japan, 117 (2009) 1285-1292.

[26] K. Midtdal, B.P. Jelle, Self-cleaning glazing products: A state-of-the-art review and future research pathways, Solar Energy Materials and Solar Cells, 109 (2013) 126-141.